

An Efficient Numerical Scheme for Simulation of Mean-reverting Square-root Diffusions*

D. DING and C. I. CHAO

Department of Mathematics, Faculty of Science and Technology, University of Macau, Macao, China, Email : dding@umac.mo

Abstract. *An efficient numerical scheme, which is based on the splitting-step idea [20], for simulation of mean-reverting square-root diffusions is presented in this paper. We prove positivity preservation for this scheme and an estimate of its local error in the second moment. A series of numerical experiments based on MATLAB programs is given to compare the suggested scheme with the schemes of the balanced implicit method (BIM) and the balanced Milstein method (BMM), which are reported in [15, 16, 19].*

Key words : Mean-reverting, square-root diffusion, simulation, positivity preservation, splitting-step algorithm.

AMS Subject Classifications : 60H35, 65C20, 65C30

1. Introduction

A mean-reverting square-root diffusion is a stochastic process X_t given by the following stochastic differential equation (SDE):

$$dX_t = \kappa(\theta - X_t)dt + \alpha\sqrt{X_t} dW_t, \tag{1}$$

where the parameters κ , θ and α are strictly positive and W_t is a standard Brownian motion defined on a filtered probability space $(\Omega, \mathcal{F}, \{\mathcal{F}_t\}, \mathbb{P})$ of standard notation. Mean-reverting square-root diffusions play a central role in several important models in finance. For instance, the mean-reverting short-time interest rate in the CIR model [6], and the variance processes in the stochastic volatility (SV) models [11].

Application of the Yamada condition (e.g. see [14]) reveals that the SDE (1) has a unique positive solution X_t for any given initial value $X_0 > 0$, which possesses the following properties [1, 2, 6, 8]:

*Work has been partially supported by the research grants RG-UL/07-08S/Y1/JXQ01/FST and RG062/08-09S/DD/FST from University of Macau.

- If $2\kappa\theta \geq \alpha^2$, then 0 is an unattainable boundary.
- If $2\kappa\theta < \alpha^2$, then 0 is an attainable boundary. In this case, 0 is strongly reflecting in this sense that the length of time spent at $X_t = 0$ is of Lebesgue measure zero.
- ∞ is an unattainable boundary.
- For each $0 \leq s < t$, the conditional distribution of X_t given X_s is a non-central chi-square distribution, and

$$\mathbb{E}[X_t \mid X_s] = \theta + (X_s - \theta) e^{-\kappa(t-s)}, \quad (2)$$

$$\mathbb{E}[X_t^2 \mid X_s] = \frac{1}{2\kappa} e^{-2\kappa(t-s)} (e^{\kappa(t-s)} - 1) (2X_s + (e^{\kappa(t-s)} - 1)\theta) (\alpha^2 + 2\kappa\theta). \quad (3)$$

Many practical applications of SV models require the introduction of Monte Carlo methods, which lead to the simulation of the mean-reverting square-root diffusions. However, this involves two problems. The first problem is that the simulation can yield negative values in a direct Euler discretization of SDE (1). The second one is that, since the square-root is not globally Lipschitzian, the convergence of the Euler scheme for SDE (1) is not guaranteed.

Recently, several authors have been concerned with positivity preservation and with efficiency of the simulation of mean-reverting square-root diffusions. Lord et al in [18] considered different Euler schemes, in particular they investigated the rules to deal with the fact that mean-reverting square-root diffusions can become negative values in a direct Euler discretization. Kahl and Jäckel in [15] analyzed and compared various numerical methods, including the balanced BIM and BMM methods. Broadie and Kaya in [3] developed a completely bias-free scheme that could simulate the Heston's SV model from its exact distribution. However, this scheme has a number of practical drawbacks, including complexity and lack of computational speed (e.g. see [1, 10]). Some approximations to exact schemes are also considered. Andersen in [1] approximated the non-central chi-square distribution by a related distribution whose moments are matched with those of the exact distribution, and then he developed two efficient schemes for the simulation of square-root diffusions. Haastrecht and Pelsser in [10] showed an accurate and efficient sampling technique for the square-root diffusions, and introduced a new and efficient simulation scheme for the Heston SV model.

In this paper, we consider a new algorithm for the simulation of the SDE (1). We decompose the SDE (1) into two equations, a SDE:

$$dY_t = \frac{1}{4}\alpha^2 dt + \alpha\sqrt{Y_t} dW_t, \quad (4)$$

and an ordinary differential equation (ODE):

$$dZ_t = \left(\kappa\theta - \kappa Z_t - \frac{1}{4}\alpha^2 \right) dt. \quad (5)$$

The idea of this decomposition comes from the splitting-step algorithm for SDEs, which was introduced by Moro and Schure in [20] to deal with the boundary preserving numerical solution of some SDEs with bounded and smooth coefficients, and also applied to study the simulations of some stochastic dynamics in mathematical finance. Some different splitting-step algorithms for RSDEs were considered and presented by Ding and Zhang in [7]. The main

advantage of the decomposition (4) and (5) is that both these two equations have exact solutions for the given initial conditions, so that it is easier to perform the practical simulation and to handle the positivity preservation problem. In fact, we can guarantee that this algorithm possesses a positivity preservation property if $4\kappa\theta \geq \alpha^2$, which meets the requirement of the most practical financial markets [15, 18].

This paper is structured as follows. After this introduction we present the efficient numerical scheme, which is based on the decomposition (4) and (5), to simulate the solution of SDE (1). We also discuss the convergence of this scheme in Section 2. Then, we give a series of numerical experiments to compare this scheme with the BIM and the BMM schemes in Section 3. Finally we make some conclusions in support of our scheme in Section 4.

2. An Efficient and Fast Algorithm

Let $T > 0$ and n be a positive integer. Denote $\Delta = T/n$, and set $t_0 = 0$ and $t_k = k\Delta$ for each $k = 1, \dots, n$, i.e. $t_0 < t_1 < \dots < t_n$ is a partition of $[0, T]$. Denote $\Delta W_{t_k} = W_{t_k} - W_{t_{k-1}}$ for $k = 1, \dots, n$. Then $\Delta W_{t_1}, \dots, \Delta W_{t_n}$ are n independent random variables having a common normal distribution with the mean 0 and the variance Δ .

We present an algorithm for SDE (1), which is based on the decomposition (4) and (5). For each $k = 1, \dots, n$, assume that we have known the value of $X_{t_{k-1}}$ of SDE (1).

1. Let $X_{t_{k-1}}$ be the initial condition. Solve the SDE (4) over $[t_{k-1}, t_k]$, i.e.

$$Y_t = X_{t_{k-1}} + \int_{t_{k-1}}^t \frac{1}{4} \alpha^2 ds + \int_{t_{k-1}}^t \alpha \sqrt{Y_s} dW_s, \quad t \in [t_{k-1}, t_k]. \quad (6)$$

2. Let Y_{t_k} be the initial condition. Solve the ODE (5) over $[t_{k-1}, t_k]$, i.e.

$$Z_t = Y_{t_k} + \int_{t_{k-1}}^t \left(\kappa\theta - \kappa Z_s - \frac{1}{4} \alpha^2 \right) ds, \quad t \in [t_{k-1}, t_k]. \quad (7)$$

Then, Z_t is used as an approximation of X_t in $[t_{k-1}, t_k]$ when $X_{t_{k-1}}$ is given.

The main advantage of this algorithm is that SDE (6) and ODE (7) have the exact solutions: By applying the Itô's formula and a transform (e.g. see Section 4.4 in [17]) we can reduce SDE (6) to a linear SDE, and then we obtain the exact solution:

$$Y_t = \left(\sqrt{X_{t_{k-1}}} + \frac{1}{2} \alpha \Delta W_t \right)^2, \quad t \in [t_{k-1}, t_k], \quad (8)$$

where $\Delta W_t = W_t - W_{t_{k-1}}$. And we can easily see the exact solution of ODE (7) is

$$Z_t = e^{-\kappa \Delta_t} Y_{t_k} + \frac{1}{\kappa} \left(\kappa\theta - \frac{1}{4} \alpha^2 \right) (1 - e^{-\kappa \Delta_t}), \quad t \in [t_{k-1}, t_k], \quad (9)$$

where $\Delta_t = t - t_{k-1}$. The following result shows that the approximation Z_t is a positivity preserving estimate for the local error.

Theorem 2.1. *Suppose that X_{t_k} is non-negative and $4\kappa\theta > \alpha^2$. The approximation Z_t is strictly positive in $[t_{k-1}, t_k]$, and its local error has the following estimate:*

$$\mathbb{E}[(X_{t_k} - Z_{t_k})^2 \mid X_{t_{k-1}}] \leq c_1 X_{t_{k-1}} \Delta + c_2 \Delta^2, \quad (10)$$

where c_1 and c_2 are positive constants which only depend on the parameters κ and θ and α , and the time T .

Proof. Equations (8) and (9) demonstrate the strict positivity of the approximation Z_{t_k} . For the given $X_{t_{k-1}}$, the SDE (1) becomes,

$$X_{t_k} = X_{t_{k-1}} + \int_{t_{k-1}}^{t_k} (\kappa\theta - \kappa X_s) ds + \int_{t_{k-1}}^{t_k} \alpha \sqrt{X_s} dW_s.$$

Combining this with equations (6) and (7) we get

$$(X_{t_k} - Z_{t_k})^2 \leq 2\kappa^2 \left(\int_{t_{k-1}}^{t_k} (X_s - Z_s) ds \right)^2 + 2\alpha^2 \left(\int_{t_{k-1}}^{t_k} (\sqrt{X_s} - \sqrt{Y_s}) dW_s \right)^2.$$

Using the Cauchy-Schwartz and the Burkholder-Davis-Cundy inequalities leads to

$$\begin{aligned} & \mathbb{E}[(X_{t_k} - Z_{t_k})^2 \mid X_{t_{k-1}}] \\ & \leq 2\kappa^2 \Delta \mathbb{E} \left[\int_{t_{k-1}}^{t_k} (X_s - Z_s)^2 ds \mid X_{t_{k-1}} \right] + 2\alpha^2 \mathbb{E} \left[\int_{t_{k-1}}^{t_k} (\sqrt{X_s} - \sqrt{Y_s})^2 ds \mid X_{t_{k-1}} \right] \\ & \leq 2\kappa^2 \Delta \int_{t_{k-1}}^{t_k} \mathbb{E}[(X_s - Z_s)^2 \mid X_{t_{k-1}}] ds + 4\alpha^2 \int_{t_{k-1}}^{t_k} (\mathbb{E}[X_s \mid X_{t_{k-1}}] + \mathbb{E}[Y_s \mid X_{t_{k-1}}]) ds. \end{aligned}$$

On the other hand, from (2) and (8), we have

$$\mathbb{E}[X_s \mid X_{t_{k-1}}] = e^{-\kappa(s-t_k)} X_{t_{k-1}} + \theta(1 - e^{-\kappa(s-t_k)}) \leq X_{t_{k-1}} + \theta \Delta,$$

and

$$\mathbb{E}[Y_s \mid X_{t_{k-1}}] = X_{t_{k-1}} + \frac{1}{4} \alpha^2 \Delta,$$

for all $s \in [t_{k-1}, t_k]$. Thus, we get

$$\mathbb{E}[(X_{t_k} - Z_{t_k})^2 \mid X_{t_{k-1}}] \leq 2\kappa^2 \Delta \int_{t_{k-1}}^{t_k} \mathbb{E}[(X_s - Z_s)^2 \mid X_{t_{k-1}}] ds + c_1 X_{t_{k-1}} \Delta + c_2 \Delta^2,$$

where $c_1 = 8\alpha^2$ and $c_2 = 4\alpha^2(\theta + \frac{1}{4}\alpha^2)$. Apply then the Gronwall's inequality to obtain

$$\begin{aligned} & \mathbb{E}[(X_{t_k} - Z_{t_k})^2 \mid X_{t_{k-1}}] \\ & \leq (c_1 X_{t_{k-1}} \Delta + c_2 \Delta^2) + (2\kappa^2 \Delta)(c_1 X_{t_{k-1}} \Delta + c_2 \Delta^2) \int_{t_{k-1}}^{t_k} e^{2\kappa^2 \Delta(t_k-s)} ds \\ & \leq (c_1 X_{t_{k-1}} \Delta + c_2 \Delta^2) + (c_1 X_{t_{k-1}} \Delta + c_2 \Delta^2) (e^{2\kappa^2 \Delta^2} - 1). \end{aligned}$$

This implies that the estimate (11) holds, and here the proof completes. ■

According to the algorithm (6) and (7), and the expressions (8) and (9), it is natural to represent a new scheme by:

$$X_k = e^{-\kappa\delta} \left(\sqrt{X_{k-1}} + \frac{1}{2} \alpha \sqrt{\Delta} \xi_k \right)^2 + \frac{1}{\kappa} \left(\kappa\theta - \frac{1}{4} \alpha^2 \right) (1 - e^{-\kappa\Delta}), \quad (11)$$

for each $k = 1, \dots, n$, where ξ_1, \dots, ξ_n are n independent random variables having a common standard normal distribution. In order to make a comparison, we also invoke the numerical schemes from the balanced implicit method, BIM, and the balanced Milstein method, BMM, for SDE (1) in the following.

The BIM scheme is defined by

$$X_k^{\text{BIM}} = X_{k-1}^{\text{BIM}} + \kappa(\theta - X_{k-1}^{\text{BIM}})\Delta + \alpha \sqrt{X_{k-1}^{\text{BIM}}} \sqrt{\Delta} \xi_k + \varphi(X_{k-1}^{\text{BIM}})(X_{k-1}^{\text{BIM}} - X_k^{\text{BIM}}), \quad (12)$$

for each $k = 1, \dots, n$, where

$$\varphi(X_{k-1}^{\text{BIM}}) = \varphi_0(X_{k-1}^{\text{BIM}})\Delta + \varphi_1(X_{k-1}^{\text{BIM}}) \sqrt{\Delta} |\xi_k|, \quad (13)$$

with the control functions:

$$\varphi_0(x) = \kappa \quad \text{and} \quad \varphi_1(x) = \begin{cases} \alpha/\sqrt{x}, & \text{if } x > \epsilon, \\ \alpha/\sqrt{\epsilon}, & \text{if } 0 \leq x \leq \epsilon, \end{cases}$$

for all $x \geq 0$, where $\epsilon > 0$ is a constant. The BIM scheme was introduced in [19], and it was shown in [21] that this scheme is able to preserve positivity of the solution of SDE (1). Also, it can only achieve the same strong order of convergence as the Euler scheme, i.e. $\frac{1}{2}$.

The BMM scheme is given by

$$\begin{aligned} X_k^{\text{BMM}} = & X_{k-1}^{\text{BMM}} + \kappa\Delta(\theta - X_{k-1}^{\text{BMM}}) + \alpha \sqrt{X_{k-1}^{\text{BMM}}} \sqrt{\Delta} \xi_k + \frac{1}{4} \alpha^2 \Delta (\xi_k^2 - 1) \\ & + \kappa\Delta(X_{k-1}^{\text{BMM}} - X_k^{\text{BMM}}), \end{aligned} \quad (14)$$

for each $k = 1, \dots, n$. It can be shown (e.g., see [16]) that the BMM scheme also preserves positivity for the SDE (1), and achieves the strong order 1 of convergence.

3. Numerical Experiments

In this section, we will compare the new scheme (New S) (11) with the BIM scheme (12) and the BMM scheme (14) via a series of numerical experiments. We consider SDE (1) in $T = 1$ and $X_0 = 0.5$ with two cases of the parameters:

- Case 1: $\alpha = 0.5$, $\theta = 0.5$ and $\kappa = 1$, i.e., $2\kappa\theta > \alpha^2$.
- Case 2: $\alpha = 0.5$, $\theta = 0.2$ and $\kappa = 0.5$, i.e., $2\kappa\theta < \alpha^2 < 4\kappa\theta$.

All numerical experiments are performed in MATLAB with the normal random number generator **randn** and **randn(m,n)**. For a detail introduction to MATLAB programs for numerical solution and simulation of SDEs, one can refer to Higham's paper [12].

First, we show that the new scheme converges to the exact solution of SDE (1). Figure 1 generates the single path simulation to SDE (1) in Case 1 for the parameters, by three schemes

with the step size $\Delta = 2^{-10}$ and using the same random numbers. It is apparent that the differences between these schemes are very slight. Tables 1 and 2 show that the errors between the new scheme and the BMM scheme under different step sizes from 2^{-10} to 2^{-6} in two respective cases for the parameters. The BMM scheme has been shown to be convergent to the exact solution of SDE (1) in [16]. Subsequently from Tables 1 and 2 we may conclude that the new scheme is also convergent. Here the errors for step sizes: $\Delta = 2^{-10}, \dots, 2^{-6}$, are given by

$$\text{error}_\Delta = \sqrt{\mathbb{E}[|X_n^{\text{BMM}} - X_n^{\text{NewS}}|^2]}, \quad (15)$$

where X_n^{BMM} and X_n^{NewS} are the respective endpoints of corresponding schemes with same step size.

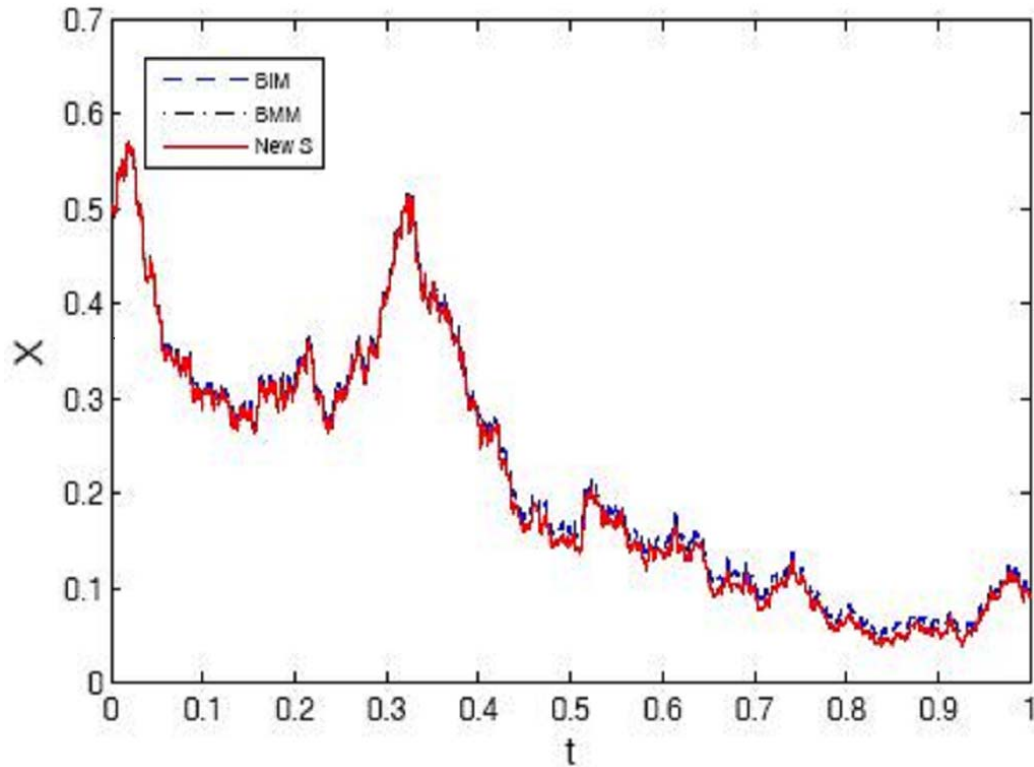


Figure 1 : Single path of (1) by using three schemes in Case 1 for the

Δ	2^{-10}	2^{-9}	2^{-8}	2^{-7}	2^{-6}
error_Δ	0.0550×10^{-3}	0.1103×10^{-3}	0.2209×10^{-3}	0.4401×10^{-3}	0.8775×10^{-3}

Table 1: Errors of different step sizes over 20000 paths in Case 1 for the parameters.

Δ	2^{-10}	2^{-9}	2^{-8}	2^{-7}	2^{-6}
error $_{\Delta}$	0.0402×10^{-3}	0.0804×10^{-3}	0.1631×10^{-3}	0.3216×10^{-3}	0.6473×10^{-3}

Table 2: Errors of different step sizes over 20000 paths in Case 2 for the parameters.

Δ	2^{-10}	2^{-9}	2^{-8}
BIM	13.016	6.125	3.047
BMM	3.531	1.593	0.797
New S	2.219	1.063	0.531

(A)

Δ	2^{-10}	2^{-9}	2^{-8}
BIM	16.219	6.297	3.125
BMM	4.062	1.672	0.828
New S	2.188	1.078	0.532

(B)

Table 3: CPU times (sec.) of three schemes over 20000 paths. (A) Case 1. (B) Case 2.

Second, Tables 3(A) and 3(B) show that the CPU times of three schemes in two cases of parameters, respectively. Here we use `tic` and `toc` in MATLAB to count the time of whole process, which starts from the first path and stops after computing the mean of the end points in these 20000 paths. From these tables, we see that the new scheme is the fastest one among these three schemes in the different cases for the parameters.

Next, we compare the convergence rates of the three schemes via estimating the order p and the constant C of

$$\epsilon_{\Delta} := \sqrt{\mathbb{E}[|X_n - X_n^{\Delta}|^2]} \approx C \cdot \Delta^p, \tag{16}$$

where, for each scheme, X_n is the endpoint with step size $\Delta = 2^{-10}$ and X_n^{Δ} are the endpoints with different step sizes $\Delta = 2^{-9}, \dots, 2^{-4}$ of same scheme. Thus, p can be considered as the convergence rate of the considered schemes. Taking logs in (16), we can plot ϵ_{Δ} against Δ on a log-log scale, and then we plot a linear least squares line:

$$\log \epsilon_{\Delta} \approx \tilde{c} + \tilde{p} \log \Delta, \tag{17}$$

to fit the points $(\log \Delta, \log \epsilon_{\Delta})$ at $\Delta = 2^{-4}, \dots, 2^{-9}$, where \tilde{c} and \tilde{p} are the least squares estimates of the constant $c = \log C$ and the slope p , respectively. Figures 2 and 3 give log-log plots for error ϵ_{Δ} , as well as their linear least squares lines, for three schemes in two respective cases for the parameters. In Figure 2, the slopes for the BIM scheme, the BMM scheme and the new scheme are 0.6069, 1.0915 and 1.1220, respectively. In Figure 3, the slopes for the BIM scheme, the BMM scheme and the new scheme are 0.5859, 1.0900 and 1.1164, respectively. In these two figures, we see that the slope of the new scheme is little better than the BMM scheme, and both of them are much better than the BIM scheme. Hence, we may conclude that the new scheme is also the most efficient among three schemes for numerical simulation of

SDE (1).

Last, we compare certain stabilities between these three schemes. Let \tilde{q} be the least squares residual of (17). Tables 4, 5 and 6 give values of \tilde{p}

	α	0.90	0.50	0.25	0.10
BIM	\tilde{p}	0.56531	0.60695	0.64927	0.69944
	\tilde{q}	0.20567	0.20425	0.18835	0.16469
BMM	\tilde{p}	0.8687	1.1035	1.1052	1.1062
	\tilde{q}	0.082626	0.16965	0.17369	0.17398
New S	\tilde{p}	0.92261	1.1258	1.123	1.1224
	\tilde{q}	0.071487	0.19938	0.19588	0.19374

Table 4: Values of \tilde{p} and \tilde{q} against different α , where $\theta = 0.5$ and $\kappa = 0.5$.

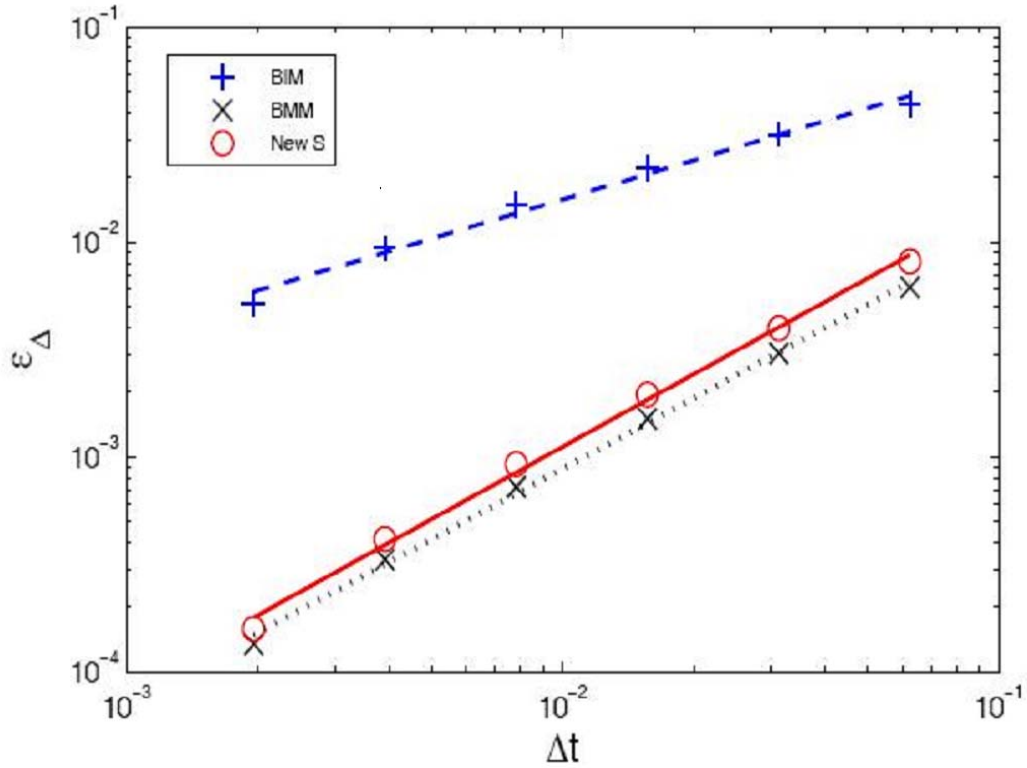


Figure 2: Log-log plots of errors for three schemes over 20000 paths with Case 1 for the parameters.

and \tilde{q} against different parameters α , θ and κ , respectively. From these tables we see that the new scheme is stable for different parameters, and still faster and more efficient than the other ones under these different parameters.

	θ	0.8	0.5	0.25	0.1
BIM	\tilde{p}	0.64801	0.62214	0.60632	0.61286
	\tilde{q}	0.19148	0.19099	0.19318	0.20527
BMM	\tilde{p}	1.1168	1.0967	1.1076	1.1341
	\tilde{q}	0.19685	0.17012	0.18116	0.22805
New S	\tilde{p}	1.1255	1.1205	1.1234	1.1254
	\tilde{q}	0.20109	0.20026	0.20193	0.20388

Table 5: Values of \tilde{p} and \tilde{q} against different θ , where $\alpha = 0.4$ and $\kappa = 0.7$.

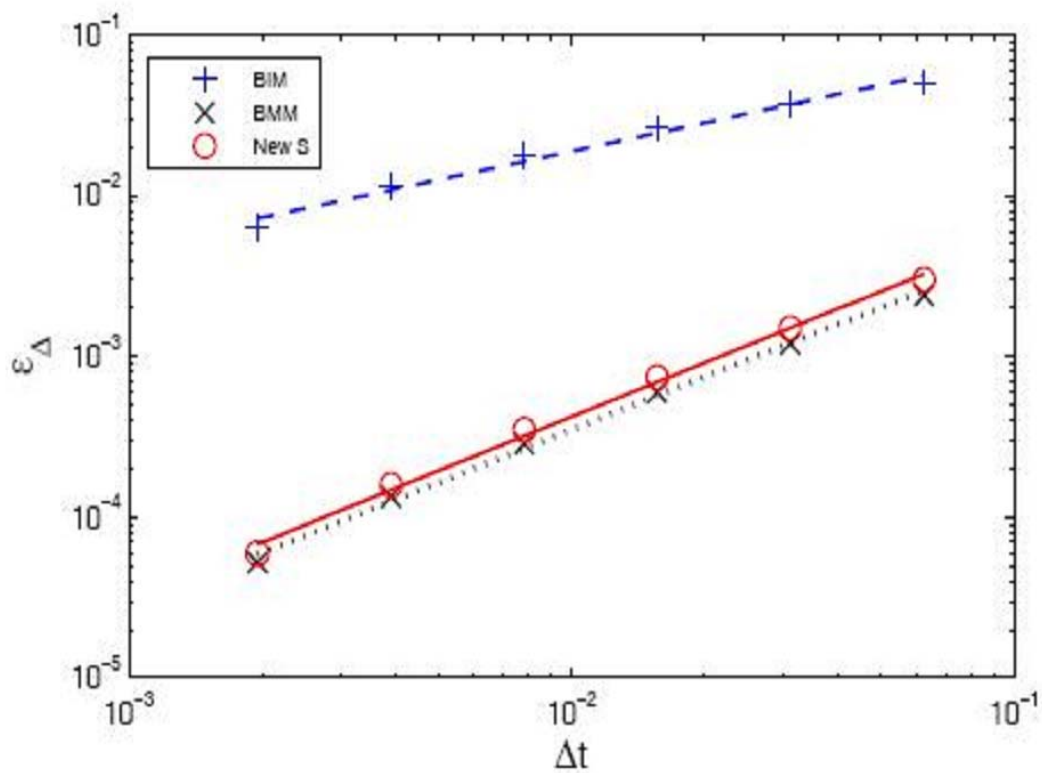


Figure 3: Log-log plots of errors for three schemes over 20000 paths with Case 2 for the parameters.

	κ	0.8	0.5	0.25	0.1
BIM	\tilde{p}	0.64441	0.63218	0.62426	0.61713
	\tilde{q}	0.18868	0.19797	0.20236	0.20624
BMM	\tilde{p}	1.1088	1.1123	1.1156	1.0789
	\tilde{q}	0.18242	0.19621	0.19233	0.13965
New S	\tilde{p}	1.1191	1.1215	1.1225	1.0878
	\tilde{q}	0.19087	0.20406	0.19956	0.14831

Table 6: Values of \tilde{p} and \tilde{q} against different κ , where $\alpha = 0.45$ and $\theta = 0.8$.

4. Some Conclusions

In this paper, we present a new scheme to numerically simulate the mean-reverting square-root diffusion, i.e. the solution of SDE (1). Our idea is based on the splitting-step method and the fact that SDE (4) and ODE (5) have the exact solutions. This scheme can preserve positivity when the parameters satisfy: $\alpha^2 \leq 4\kappa\theta$. Furthermore, via numerical experiments, this scheme is also shown to be more efficient and faster than the BIM and BMM schemes. Actually, in order to maintain precision when applying Monte-Carlo methods, one needs to use a large numbers of paths. Hence saving time becomes the most important factor when addressing the pertaining problem. Our new scheme is illustrated in this respect to provide for good efficiency and much time saving. The estimate of the local error of this new scheme, in the 2nd moment, is thought to partially guarantee that this scheme is theoretically convergent.

References

- [1] L. Andersen, Efficient simulation of the Heston stochastic volatility model, <http://ssrn.com/abstract=946405>, *Bank of American Securities*, 2007.
- [2] L. Andersen, and V. V. Piterbarg, Moment explosions in stochastic volatility models, *Finance & Stochastics* **11**, (2007), 29–50.
- [3] M. Broadie, and Ö. Kaya, Exact simulation of stochastic volatility and other affine jump diffusion processes, *Operations Research* **54**, (2006), 217–231.
- [4] P. Carr, H. Geman, D.B. Madan, and M. Yor, Stochastic volatility for Lévy processes, *Mathematical Finance* **13**, (2003), 345–382.
- [5] R. Cont, and P. Tankov, *Financial Modelling with Jump Processes*, Chapman & Hall/CRC Press, 2003.
- [6] J. C. Cox, J. E. Ingersoll, and S. A. Ross, A theory of the term structure of interest rates, *Econometrica* **53**, (1985), 385–408.
- [7] D. Ding, and Y. Y. Zhang, A splitting-step algorithm for reflected stochastic differential

equations in \mathbb{R}_+^1 , *Computers & Mathematics with Applications* **55**, (2008), 2413–2425.

[8] D. Dufresne, The integrated square-root process, R. P. 90,

<http://repository.unimelb.edu.au/10187/1413>, Univ. of Melbourne, Australia, 2001.

[9] P. Glasserman, *Monte Carlo Methods in Financial Engineering*, Spring-Verlag, NY, 2004.

[10] A. von Haastrecht, and A. Pelesser, Efficient, almost exact simulation of the Heston stochastic volatility model, <http://ssrn.com/abstract=1131137>, 2008.

[11] S. Heston, A closed form solution for options with stochastic volatility with applications to bond and currency options, *The Review of Financial Studies* **6**, (1993), 327–343.

[12] D. J. Higham, An algorithmic introduction to numerical simulation of stochastic differential equations, *SIAM Review* **43**, (2001), 525–546.

[13] D. J. Higham, and X. Mao, Convergence of Monte Carlo simulations involving the mean-reverting square root process, *Journal of Computational Finance* **8**, (2005), 101–119.

[14] I. Karatzas, and S. E. Shreve, *Brownian Motion and Stochastic Calculus, 2nd Ed.*, Springer-Verlag, New York, 1991.

[15] C. Kahl, and P. Jäckel, Fast strong approximation Monte-Carlo schemes for stochastic volatility models, *Quantitative Finance* **6**, (2006), 513–536.

[16] C. Kahl, and H. Schurz, Balanced Milstein methods for ordinary SDEs, *Monte Carlo Methods & Applications* **12**, (2006), 143–170.

[17] P. E. Kloeden, and E. Platen, *Numerical Solution of Stochastic Differential Equations*, Springer-Verlag, New York, 1995.

[18] R. Lord, R. Koekkoek, and D. van Dijk, A comparison of biased simulation schemes for stochastic volatility models, <http://ssrn.com/abstract=903116>, Tinbergen Institute, 2006.

[19] G. N. Milstein, E. Platen, and H. Schurz, Balanced implicit methods for stiff stochastic systems, *SIAM Journal on Numerical Analysis* **38**, (1998), 1010–1019.

[20] E. Moro, and H. Schurz, Boundary preserving semi-analytical numerical algorithms for stochastic differential equations, *SIAM Journal on Scientific Computing* **29**, (2007), 1525–1549.

[21] H. Schurz, Numerical regularization for SDE's: Construction of nonnegative solutions, *Dynamical Systems & Applications* **5**, (1996), 323–352.

[22] R. D. Smith, An almost exact simulation method for the Heston model, *Journal of Computational Finance* **11**, (2007), 115–125.